Tritium β decay in chiral effective field theory

A. Baroni,[1] L. Girlanda,[2,3] A. Kievsky,[4] L. E. Marcucci,[4,5] R. Schiavilla,[1,6] and M. Viviani[4]
[1]*Department of Physics, Old Dominion University, Norfolk, Virginia 23529, USA*
[2]*Department of Mathematics and Physics, University of Salento, 73100 Lecce, Italy*
[3]*INFN-Lecce, 73100 Lecce, Italy*
[4]*INFN-Pisa, 56127 Pisa, Italy*
[5]*Department of Physics, University of Pisa, 56127 Pisa, Italy*
[6]*Theory Center, Jefferson Lab, Newport News, Virginia 23606, USA*
(Received 5 May 2016; revised manuscript received 12 July 2016; published 18 August 2016)

We evaluate the Fermi and Gamow-Teller (GT) matrix elements in tritium β decay by including in the charge-changing weak current the corrections up to one loop recently derived in nuclear chiral effective field theory (χEFT). The trinucleon wave functions are obtained from hyperspherical-harmonics solutions of the Schrödinger equation with two- and three-nucleon potentials corresponding to either χEFT (the N3LO/N2LO combination) or meson-exchange phenomenology (the AV18/UIX combination). We find that contributions due to loop corrections in the axial current are, in relative terms, as large as (and in some cases, dominate) those from one-pion exchange, which nominally occur at lower order in the power counting. We also provide values for the low-energy constants multiplying the contact axial current and three-nucleon potential, required to reproduce the experimental GT matrix element and trinucleon binding energies in the N3LO/N2LO and AV18/UIX calculations.

DOI: 10.1103/PhysRevC.94.024003

I. INTRODUCTION

Recently, nuclear axial current and charge operators have been derived in chiral effective field theory (χEFT) up to one loop in a formalism based on time-ordered perturbation theory, in which, along with irreducible contributions, noniterative terms in reducible contributions were identified and accounted for order-by-order in the power counting [1]. Ultraviolet divergencies associated with the loop corrections were isolated in dimensional regularization. The resulting axial current was found to be finite and conserved in the chiral limit, while the axial charge required renormalization. In particular, the divergencies in the loop corrections to the one-pion exchange axial charge were reabsorbed by renormalization of some of the low-energy constants (LECs) d_i characterizing the subleading πN Lagrangian $\mathcal{L}^{(3)}_{\pi N}$ [2]. For a detailed discussion of these issues (formalism, renormalization, etc.) we defer to Ref. [1]. However, a brief summary is provided in the next section.

In the present paper, the focus is on the axial current, whose contributions up to one loop are illustrated diagrammatically in Fig. 1. Pion-pole terms are crucial for the current to be conserved in the chiral limit [1]—these terms were ignored in the earlier studies of Park *et al.* [3,4]; of course, they are suppressed in low momentum transfer processes such as the tritium β decay under consideration here. Vertices involving three or four pions, such as those, for example, occurring in panels (l), (p), (q), and (r) of Fig. 1, depend on the pion field parametrization. This dependence must cancel out after summing the individual contributions associated with these diagrams, as indeed it does [1] (this and the requirement that the axial current be conserved in the chiral limit provide useful checks of the calculation).

In Fig. 1 the labeling NnLO corresponds to the power counting $Q^n \times Q^{\rm LO}$, where Q denotes generically the low momentum scale and $Q^{\rm LO}$ is Q^{-3} for the axial current [1]. The LO and N2LO currents consist of single-nucleon terms; the N2LO current includes relativistic corrections proportional to $1/m^2$ (m is the nucleon mass), suppressed by two powers of Q relative to the LO. Pion-range currents contribute at N3LO, panels (e) and (f) of Fig. 1, and involve vertices from the subleading $\mathcal{L}^{(2)}_{\pi N}$ chiral Lagrangian [2], proportional to the LECs c_3, c_4, and c_6. At this order (N3LO) there is also a contact current proportional to a single LEC, which we denote as z_0 following Ref. [1]. This LEC is related to the LEC c_D (in standard notation), which enters the three-nucleon chiral potential at leading order. The two LECs c_D and c_E which fully characterize this potential have recently been constrained by reproducing the empirical value of the Gamow-Teller (GT) matrix element in tritium β decay and the binding energies of the trinucleons [5,6]. However, the value determined for z_0 in those earlier studies was based on calculations which retained only terms up to N3LO in the axial current. As a matter of fact, one of the goals of the present work is to provide a determination of z_0 by also accounting for the N4LO corrections, represented by diagrams (i)–(x) in Fig. 1.

Most calculations of nuclear axial current matrix elements, such as those reported for the pp and $p\,^3$He weak fusions of interest in solar physics in Refs. [4,7], and for muon capture on ^{2}H and ^{3}He in Ref. [6], have ignored these N4LO corrections. One exception is Ref. [8], which included effective one-body reductions, for use in a shell-model study, of some of the two-pion exchange terms derived in Ref. [4]. However, a systematic study of axial current contributions at N4LO is still lacking. The other goal of the present work is to provide a numerically exact estimate of these contributions in the ^{3}H GT matrix element.

II. FORMALISM

The starting point of the derivation of nuclear current operators is the chiral Lagrangian for interacting pions and

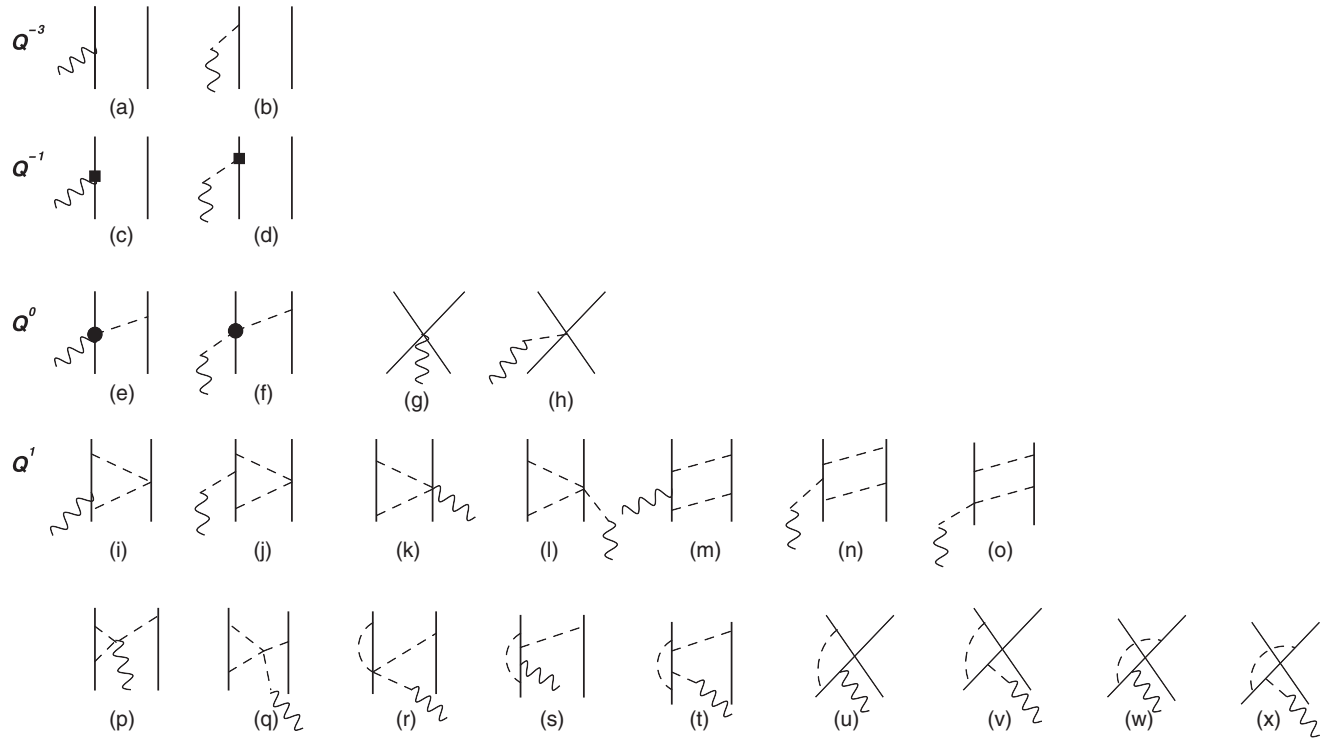

FIG. 1. Diagrams illustrating the one- and two-body axial currents entering at order Q^{-3} (LO), Q^{-1} (N2LO), Q^{0} (N3LO), and Q^{1} (N4LO), where Q denotes generically the low-momentum scale. Nucleons, pions, and axial fields are denoted by solid, dashed, and wavy lines, respectively. The squares in (c) and (d) denote relativistic corrections to the one-body axial current, while the circles in (e) and (f) represent vertices implied by the $\mathcal{L}^{(2)}_{\pi N}$ chiral Lagrangian, involving the LECs c_i (see Ref. [1] for additional explanations). Only a single time ordering is shown; in particular, all direct- and crossed-box diagrams are accounted for. The contributions associated with diagrams (w) and (x) were overlooked in Ref. [1].

nucleons. This defines a quantum field theory which satisfies, besides all common general properties, like unitarity, analyticity, crossing symmetry and cluster decomposition, all constraints from chiral symmetry, in the form of chiral Ward identities, e.g., (partial) current conservation. Due to the (pseudo-)Goldstone boson character of the pions, their interactions can be organized according to increasing powers of their momenta, whose magnitude is generically denoted Q, much smaller than the hadronic scale $\Lambda_\chi \sim 1$ GeV. From the chiral Lagrangian one can derive, in the canonical formalism, the chiral Hamiltonian, divided into a free part H_0 and an interacting part H_I, which allows one to calculate transition amplitudes by applying the rules of time-ordered perturbation theory (TOPT),

$$\langle f \mid T \mid i\rangle = \langle f \mid H_I \sum_{n=1}^{\infty} \left(\frac{1}{E_i - H_0 + i\,\eta} H_I \right)^{n-1} \mid i\rangle. \quad (1)$$

The evaluation of this amplitude is in practice carried out by inserting complete sets of H_0 eigenstates between successive terms of H_I. Power counting is then used to organize the diagrammatic expansion (which in general will involve reducible—i.e., with purely nucleonic intermediate states—and irreducible contributions) in powers of $(Q/\Lambda_\chi) \ll 1$. In this expansion we also take into account non-static contributions which represent nucleon-recoil corrections, by expanding a generic energy denominator as

$$\frac{1}{E_i - E_I - \omega_\pi} = -\frac{1}{\omega_\pi}\left[1 + \frac{E_i - E_I}{\omega_\pi} + \frac{(E_i - E_I)^2}{\omega_\pi^2} + \dots\right], \quad (2)$$

where E_I denotes the kinetic energy of the intermediate purely-nucleonic state, ω_π the pion energy (or energies, as the case may be), and the ratio $(E_i - E_I)/\omega_\pi$ is of order Q. As a result the scattering amplitude T admits the following expansion:

$$T = T^{(n)} + T^{(n+1)} + T^{(n+2)} + \dots, \quad (3)$$

where $T^{(m)} \sim Q^m$, and chiral symmetry ensures that n is finite. In the case of the two-nucleon amplitude $n = 0$. Obviously, an infinite set of contributions to the TOPT expansion must be resummed in order to describe nuclear bound states. This is achieved by defining a kernel that satisfies a Lippmann-Schwinger (LS) equation and generates the above perturbative expansion of the scattering amplitude. Thus, a two-nucleon potential v can be derived, assumed to admit the same kind of low-energy expansion as in Eq. (3), which when iterated in the LS equation,

$$v + v\,G_0\,v + v\,G_0\,v\,G_0\,v + \dots, \quad (4)$$

where G_0 denotes the free two-nucleon propagator $G_0 = 1/(E_i - E_I + i\,\eta)$, leads to the on-the-energy-shell $(E_i = E_f)$

T matrix in Eq. (3), up to any specified order in the power counting. In this way one obtains

$$v^{(0)} = T^{(0)}, \tag{5}$$

$$v^{(1)} = T^{(1)} - [v^{(0)}\, G_0\, v^{(0)}], \tag{6}$$

$$v^{(2)} = T^{(2)} - [v^{(0)}\, G_0\, v^{(0)}\, G_0\, v^{(0)}] - [v^{(1)}\, G_0\, v^{(0)} + v^{(0)}\, G_0\, v^{(1)}]. \tag{7}$$

Notice that a term like $v^{(m)} G_0 v^{(n)}$ is of order Q^{m+n+1}, since G_0 is of order Q^{-2} and the implicit loop integration brings in a factor Q^3. The leading-order (LO) Q^0 term, $v^{(0)}$, consists of two (nonderivative) contact interactions and (static) one-pion exchange (OPE) [respectively displayed in panels (a′) and (b′), of Fig. 2], while the next-to-leading (NLO) Q^1 term, $v^{(1)}$, is easily seen to vanish [9], since the leading nonstatic corrections $T^{(1)}$ to the (static) OPE amplitude add up to zero on the energy shell, while the remaining diagrams in $T^{(1)}$ represent iterations of $v^{(0)}$, whose contributions are exactly canceled by $[v^{(0)}\, G_0\, v^{(0)}]$ (complete or partial cancellations of this type persist at higher $n \geqslant 2$ orders). The next-to-next-to-leading (N2LO) Q^2 term, which follows from Eq. (7), contains contact (involving two gradients of the nucleon fields) interactions, two-pion-exchange (TPE), loop corrections to LO contact interactions, and loop corrections to OPE potential [respectively displayed in panels (c′), (d′)–(f′), (g′) and (h′), and (i′), of Fig. 2]. However, the procedure outlined above does not specify the potential uniquely, being affected by well known off energy-shell ambiguities. Indeed, at N2LO there is also a recoil correction to the OPE, which we write as [10]

$$v_\pi^{(2)}(\nu) = v_\pi^{(0)}(\mathbf{k})\, \frac{(1-\nu)[(E_1' - E_1)^2 + (E_2' - E_2)^2] - 2\,\nu\,(E_1' - E_1)(E_2' - E_2)}{2\,\omega_k^2}, \tag{8}$$

where $v_\pi^{(0)}(\mathbf{k})$ is the leading order OPE potential, defined as

$$v_\pi^{(0)}(\mathbf{k}) = -\frac{g_A^2}{4\,f_\pi^2}\, \boldsymbol{\tau}_1 \cdot \boldsymbol{\tau}_2\; \boldsymbol{\sigma}_1 \cdot \mathbf{k}\; \boldsymbol{\sigma}_2 \cdot \mathbf{k}\, \frac{1}{\omega_k^2}, \tag{9}$$

E_i ($\mathbf{p}_i$) and E_i' ($\mathbf{p}_i'$) are the initial and final energies (momenta) of nucleon i, and $\mathbf{k} = \mathbf{p}_1 - \mathbf{p}_1'$. There is an infinite class of corrections $v_\pi^{(2)}(\nu)$, labeled by the parameter ν, which, while equivalent on the energy shell ($E_1' + E_2' = E_1 + E_2$) and hence independent of ν, are different off the energy shell. Friar [10] has in fact shown that these different off-the-energy-shell extrapolations $v_\pi^{(2)}(\nu)$ are unitarily equivalent, and thus do not affect physical observables. The off-shell ambiguity propagates to the next-order $v^{(3)}$, but the unitary equivalence persists also at this order, i.e., at the two-pion exchange level [9].

The inclusion (in first order) of electroweak interactions in the perturbative expansion of Eq. (1) is, in principle, straightforward. The weak transition operator can be expanded as [1,9]

$$T_5 = T_5^{(n)} + T_5^{(n+1)} + T_5^{(n+2)} + \ldots, \tag{10}$$

where $T_5^{(m)}$ is of order Q^m and $n = -3$ in this case. The nuclear weak axial charge, $\rho_{5,a}$, and current, $\mathbf{j}_{5,a}$, operators follow from $v_5 = A_a^0\, \rho_{5,a} - \mathbf{A}_a \cdot \mathbf{j}_{5,a}$, where $A_a^\mu = (A_a^0, \mathbf{A}_a)$ is the weak axial field, and it is assumed that v_5 has a similar expansion as T_5. The requirement that, in the context of the LS equation, v_5 matches T_5 order by order in the power counting implies relations for $v_5^{(n)} = A_a^0\, \rho_{5,a}^{(n)} - \mathbf{A}_a \cdot \mathbf{j}_{5,a}^{(n)}$, which can be found in Refs. [1,9], similar to those derived above for $v^{(n)}$, the strong-interaction potential. The lowest order terms that contribute to the axial current operators have $n = -3$, while $n = -2$ for the axial charge. This implies that the off-shell ambiguity affects the axial current already at N3LO and the axial charge at N4LO. In the case of the electromagnetic operators the same was true with inverted roles of the charge and current [9]. There it was shown that different choices for the ν parameter for both the potential and the electromagnetic charge operator were unitarily equivalent. We expect the same to occur for the axial current, although this has not been verified explicitly. The specific form of the axial current we use corresponds to the choice $\nu = 0$ for $v_\pi^{(2)}(\nu)$ and $v_{2\pi}^{(3)}(\nu)$, specifically Eq. (8) above and Eq. (19) of Ref. [9]. The remaining nonstatic corrections in the potential $v^{(3)}$ are as given in Eqs. (B8), (B10), and (B12) of that work.

We notice that at N4LO there are several one loop diagrams that contribute to the nuclear axial current. Diagrams (k), (l), (p), (q), and (r) of Fig. 1 are irreducible and in Ref. [1] they were shown to give the same contribution both in TOPT and heavy-baryon perturbation theory (HBPT). The remaining topologies contain reducible diagrams and require the subtraction of the iterations generated by the LS equation [1,9,11]. The partially conserved axial current (PCAC) relation implies the conservation of the weak axial current in the chiral limit $\mathbf{q} \cdot \mathbf{j}_{5,a} = [\, H, \rho_{5,a}\,]$ with the two-nucleon Hamiltonian given by $H = T^{(-1)} + v^{(0)} + v^{(2)} + \cdots$ and where the (two-nucleon) kinetic energy $T^{(-1)}$ is counted as Q^{-1}. This requirement, order by order in the power counting, translates into a set of nontrivial relations between the $\mathbf{j}_{5,a}^{(n)}$ and the $T^{(-1)}$, $v^{(n)}$, and $\rho_{5,a}^{(n)}$ (note that commutators implicitly bring in factors of Q^3), see Eqs. (7.9)–(7.12) of Ref. [1]. These relations couple contributions of different orders in the power counting of the operators, and can only be satisfied up to a truncation of the low-energy expansion. In Ref. [1] it has been shown that the axial current, up to order Q, is conserved in the chiral limit. In particular we note that the sum of the loop corrections at order Q displayed in Fig. 1, when contracted with the three-momentum $\mathbf{q}$ of the external axial field, is equal to the following commutator:

$$\left[\, v_\pi^{(0)},\quad \rho_{5,a}^{(-1)}\right], \tag{11}$$

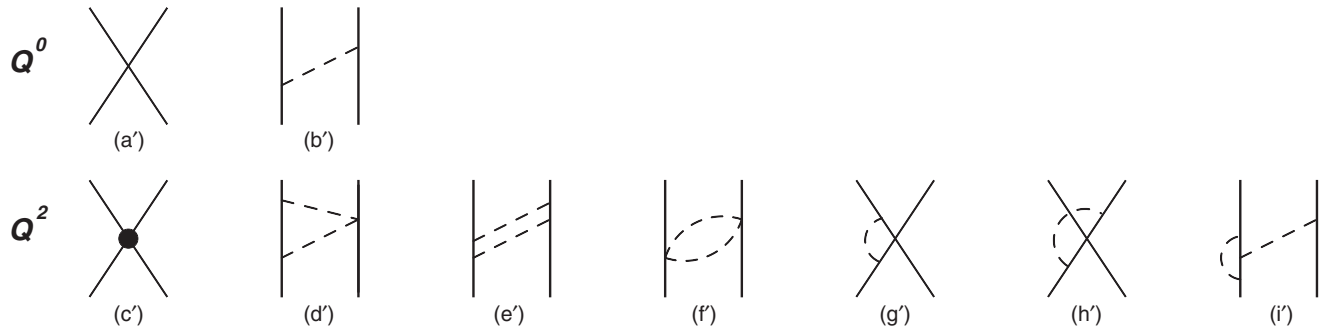

FIG. 2. Diagrams illustrating contributions to the two-nucleon potential entering at Q^0, (a′) and (b′), and at Q^2, (c′)–(i′). Nucleons and pions are denoted by solid and dashed lines, respectively. The filled circle in (c′) represents the vertex from contact Hamiltonians containing two gradients of the nucleons' field. Vertex corrections coming from $\mathcal{L}^{(3)}_{\pi N}$ as well as $1/m$ corrections to the vertices and energy denominators, entering at order Q^2, are not displayed. Only a single time ordering for each topology is shown. In particular all direct- and crossed-box diagrams are accounted for.

where $v_\pi^{(0)}$ is the OPE potential, panel (b′) of Fig. 2, and $\rho_{5,a}^{(-1)}$ is the LO two-body axial charge. Finally we note that the verification of PCAC, for nonvanishing pion mass, should come out as a natural consequence of the fact that we used chiral Lagrangians without making any approximations (besides neglecting some $1/m$ corrections at order Q, for further details we defer to Sec IV B of Ref. [1]). However an explicit verification of PCAC for tree level diagrams as well as loop corrections at order Q of Fig. 1 has not yet been performed.

III. NUCLEAR AXIAL CURRENTS IN χEFT

In this section we report the expressions for the nuclear axial current in the limit of vanishing external field momentum (denoted as $\mathbf{q}$) [1]. Of course, pion-pole contributions in Fig. 1 vanish in this limit. The expressions at LO and N2LO read

$$\mathbf{j}^{\rm LO}_{\pm} = -g_A\,\tau_{1,\pm}\,\boldsymbol{\sigma}_1 + (1 \rightleftharpoons 2), \tag{12}$$

$$\mathbf{j}^{\rm N2LO}_{\pm} = \frac{g_A}{2m^2}\,\tau_{1,\pm}\big(K_1^2\,\boldsymbol{\sigma}_1 - \mathbf{K}_1\;\boldsymbol{\sigma}_1\cdot\mathbf{K}_1\big) + (1 \rightleftharpoons 2), \tag{13}$$

while those at N3LO are separated into one-pion exchange (OPE) and contact (CT) terms corresponding, respectively, to panels (e) and (g) of Fig. 1:

$$\begin{aligned}\mathbf{j}^{\rm N3LO}_{\pm}({\rm OPE};\mathbf{k}) = \frac{g_A}{2\,f_\pi^2}\Big\{&4\,c_3\,\tau_{2,\pm}\,\mathbf{k} + (\boldsymbol{\tau}_1\times\boldsymbol{\tau}_2)_\pm \\ &\times\left[\left(c_4+\frac{1}{4\,m}\right)\boldsymbol{\sigma}_1\times\mathbf{k} - \frac{i}{2\,m}\mathbf{K}_1\right]\Big\} \\ &\times\boldsymbol{\sigma}_2\cdot\mathbf{k}\,\frac{1}{\omega_k^2} + (1 \rightleftharpoons 2),\end{aligned} \tag{14}$$

$$\mathbf{j}^{\rm N3LO}_{\pm}({\rm CT};\mathbf{k}) = z_0\,(\boldsymbol{\tau}_1\times\boldsymbol{\tau}_2)_\pm\,\boldsymbol{\sigma}_1\times\boldsymbol{\sigma}_2. \tag{15}$$

The LECs c_3 and c_4 in the OPE current effectively include the contributions associated with Δ-isobar excitations (Δ degrees of freedom are integrated out in the χEFT formulation adopted here) as well as short-range contributions involving vector meson exchanges, such as axial $\rho-\pi$ transition mechanisms [4].

Lastly, the expressions at N4LO are separated into terms originating from OPE, panel (s), and multipion exchange (MPE), panels (i), (k), (m), and (p):

$$\begin{aligned}\mathbf{j}^{\rm N4LO}_{\pm}({\rm OPE};\mathbf{k}) = \frac{g_A^5\,m_\pi}{256\,\pi\,f_\pi^4}&[18\tau_{2,\pm}\,\mathbf{k} - (\boldsymbol{\tau}_1\times\boldsymbol{\tau}_2)_\pm\boldsymbol{\sigma}_1\times\mathbf{k}] \\ &\times\boldsymbol{\sigma}_2\cdot\mathbf{k}\,\frac{1}{\omega_k^2} + (1 \rightleftharpoons 2),\end{aligned} \tag{16}$$

$$\begin{aligned}\mathbf{j}^{\rm N4LO}_{\pm}({\rm MPE};\mathbf{k}) = &\frac{g_A^3}{32\,\pi f_\pi^4}\,\tau_{2,\pm}\Big[W_1(k)\,\boldsymbol{\sigma}_1 + W_2(k)\,\mathbf{k}\;\boldsymbol{\sigma}_1 \\ &\cdot\mathbf{k} + Z_1(k)\left(2\,\mathbf{k}\;\boldsymbol{\sigma}_2\cdot\mathbf{k}\,\frac{1}{\omega_k^2} - \boldsymbol{\sigma}_2\right)\Big] \\ &+ \frac{g_A^5}{32\,\pi f_\pi^4}\,\tau_{1,\pm}\,W_3(k)(\boldsymbol{\sigma}_2\times\mathbf{k})\times\mathbf{k} \\ &- \frac{g_A^3}{32\,\pi f_\pi^4}(\boldsymbol{\tau}_1\times\boldsymbol{\tau}_2)_\pm Z_3(k)\,\boldsymbol{\sigma}_1\times\mathbf{k} \\ &\times\boldsymbol{\sigma}_2\cdot\mathbf{k}\,\frac{1}{\omega_k^2} + (1 \rightleftharpoons 2),\end{aligned} \tag{17}$$

where the loop functions are given by

$$\begin{aligned}W_1(k) = \int_0^1 dz\Big[&\big(1-5\,g_A^2\big)M(k,z) \\ &- \frac{g_A^2\,k^2}{2}\left[\frac{9\,z\,\bar z-1}{M(k,z)} - \frac{k^2(z\,\bar z)^2}{M(k,z)^3}\right]\Big],\end{aligned} \tag{18}$$

$$W_2(k) = \int_0^1 dz\left[-\frac{g_A^2\,(z\,\bar z)^2\,k^2}{2\,M(k,z)^3} + \frac{z\,\bar z\big(7\,g_A^2+2\big) - g_A^2}{2M(k,z)}\right], \tag{19}$$

$$W_3(k) = -\frac{1}{2}\int_0^1 dz\left[\frac{k^2\,(z-\bar z)^2}{12\,M(k,z)^3} + \frac{1}{M(k,z)}\right], \tag{20}$$

$$Z_1(k) = \int_0^1 dz\left[\frac{z\,\bar z\,k^2}{M(k,z)} + 3\,M(k,z)\right], \tag{21}$$

$$Z_3(k) = \int_0^1 dz\,M(k,z), \tag{22}$$

and

$$M(k,z) = \sqrt{z\bar{z}\,k^2 + m_\pi^2}, \qquad \bar{z} = 1 - z. \tag{23}$$

In the equations above, g_A and f_π are the nucleon axial coupling constant and pion decay amplitude, m and m_π are the nucleon and pion mass, $\omega_k = \sqrt{k^2 + m_\pi^2}$ is the pion energy, and c_3, c_4, and z_0 are LECs, c_3 and c_4 entering the $\mathcal{L}^{(2)}_{\pi N}$ Lagrangian and z_0 multiplying the contact axial current (these LECs are discussed in Sec. IV). The nucleon spin and isospin operators are denoted by $\boldsymbol{\sigma}$ and $\boldsymbol{\tau}$, respectively, and the following charge-raising (+) and charge-lowering (−) combinations have been defined:

$$\begin{aligned} \tau_{i,\pm} &= (\tau_{i,x} \pm i\,\tau_{i,y})/2, \\ (\boldsymbol{\tau}_1 \times \boldsymbol{\tau}_2)_\pm &= (\boldsymbol{\tau}_1 \times \boldsymbol{\tau}_2)_x \pm i\,(\boldsymbol{\tau}_1 \times \boldsymbol{\tau}_2)_y. \end{aligned} \tag{24}$$

The momenta $\mathbf{k}_i$ and $\mathbf{K}_i$ are

$$\mathbf{k}_i = \mathbf{p}_i' - \mathbf{p}_i, \qquad \mathbf{K}_i = \left(\mathbf{p}_i' + \mathbf{p}_i\right)/2, \tag{25}$$

where $\mathbf{p}_i$ ($\mathbf{p}_i'$) is the nucleon initial (final) momentum and, in the limit of vanishing external field momentum, $\mathbf{k}_1$ and $\mathbf{k}_2$ are related via

$$\mathbf{k}_1 = \mathbf{k} = -\mathbf{k}_2. \tag{26}$$

In Ref. [1] diagrams (w) and (x) of Fig. 1 were inadvertently omitted, only diagrams (u) and (v) were considered. We have evaluated them here, and obtained for the combined contribution of (u) and (w) the N4LO contact current

$$\begin{aligned} \text{diagrams (u)} + \text{(w)} = -\frac{g_A^3\, m_\pi}{16\,\pi\, f_\pi^2}\, C_T\, [4\,(\tau_{1,\pm} - \tau_{2,\pm})\,\boldsymbol{\sigma}_2 \\ + (\boldsymbol{\tau}_1 \times \boldsymbol{\tau}_2)_\pm (\boldsymbol{\sigma}_1 \times \boldsymbol{\sigma}_2)] + (1 \rightleftharpoons 2), \end{aligned} \tag{27}$$

where C_T (in standard notation) is one of the two LECs in the four-nucleon contact interaction at LO. The pion-pole contribution from diagrams (v)+(x) follows as

$$\text{diagrams (v)} + \text{(x)} = -\frac{\mathbf{q}}{q^2 + m_\pi^2}\,\mathbf{q}\cdot\big[\text{diagrams (u)} + \text{(w)}\big]. \tag{28}$$

However, use of Fierz identities shows that the contact current in Eq. (27) vanishes identically [1].

In a three-nucleon system the two-body loop corrections to the axial current enter at order Q^{-2}, owing to the presence of a momentum-conserving δ function $\delta(\mathbf{p}_3' - \mathbf{p}_3)$. These loop corrections turn out to be of the same order as the three-body axial current, illustrated in Fig. 3 and first derived in Ref. [4]:

$$\begin{aligned} &\mathbf{j}_\pm^{\rm N4LO}(3\mathrm{B};\mathbf{k}_2,\mathbf{k}_3) \\ &= -\sum_{\rm cyc} \frac{g_A^3}{8\,f_\pi^4}(2\,\tau_{1,\pm}\,\boldsymbol{\tau}_2\cdot\boldsymbol{\tau}_3 - \tau_{2,\pm}\,\boldsymbol{\tau}_3\cdot\boldsymbol{\tau}_1 - \tau_{3,\pm}\,\boldsymbol{\tau}_1\cdot\boldsymbol{\tau}_2) \\ &\quad\times\left(\boldsymbol{\sigma}_1 - \frac{4}{3}\frac{\boldsymbol{\sigma}_1\cdot\mathbf{k}_1\,\mathbf{k}_1}{\omega_1^2}\right)\frac{\boldsymbol{\sigma}_2\cdot\mathbf{k}_2}{\omega_2^2}\frac{\boldsymbol{\sigma}_3\cdot\mathbf{k}_3}{\omega_3^2}, \end{aligned} \tag{29}$$

where the sum is over the cyclic permutations of the three nucleons, and in the $\mathbf{q} = 0$ limit $\mathbf{k}_1 = -(\mathbf{k}_2 + \mathbf{k}_3)$.

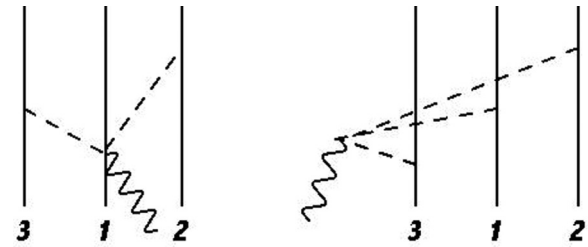

(a) (b)

FIG. 3. Diagrams illustrating the three-body axial current at N4LO (i.e., order Q^{-2} in a three-nucleon system). Nucleons, pions, and axial fields are denoted by solid, dashed, and wavy lines, respectively. Only a single time ordering is shown and pion-pole contributions are ignored.

Configuration-space expressions for these two- and three-body operators (denoted generically as 2B and 3B, respectively) follow from

$$\mathbf{j}_\pm(2\mathrm{B}) = \int \frac{d\mathbf{k}}{(2\pi)^3}\, e^{i\mathbf{k}\cdot\mathbf{r}_{12}}\, C_\Lambda(k)\, \mathbf{j}(2\mathrm{B};\mathbf{k}), \tag{30}$$

$$\begin{aligned} \mathbf{j}_\pm(3\mathrm{B}) = \int \frac{d\mathbf{k}_2}{(2\pi)^3}\frac{d\mathbf{k}_3}{(2\pi)^3}\, e^{-i\mathbf{k}_2\cdot\mathbf{r}_{12}}\, e^{-i\mathbf{k}_3\cdot\mathbf{r}_{13}} \\ \times C_\Lambda(k_2)\, C_\Lambda(k_3)\, \mathbf{j}(3\mathrm{B};\mathbf{k}_2,\mathbf{k}_3), \end{aligned} \tag{31}$$

where the relative positions are defined as $\mathbf{r}_{ij} = \mathbf{r}_i - \mathbf{r}_j$, and $C_\Lambda(k)$ is the momentum cutoff, which we take as

$$C_\Lambda(k) = e^{-(k/\Lambda)^4}. \tag{32}$$

This cutoff does not modify the power counting of the various terms, as it is easily seen by expanding in powers of k/Λ. In particular, the conservation of the vector current and axial current (in the chiral limit) is preserved up to the order considered in the present work.

Lastly, terms proportional to $\mathbf{K}_j$ in the N2LO and N3LO currents are obtained by replacing $\mathbf{K}_j$ with $-i\,\boldsymbol{\nabla}_j$ in configuration space (the momentum operator), and need to be symmetrized accordingly to preserve Hermiticity. Explicit expressions for these Fourier transforms are listed in the Appendix.

IV. GAMOW-TELLER MATRIX ELEMENT IN TRITIUM β DECAY

The Gamow-Teller (GT) matrix element is obtained from the tritium half-life via (see [12] and references therein)

$$(1 + \delta_R)\, t\, f_V = \frac{K/G_V^2}{\langle\mathbf{F}\rangle^2 + f_A/f_V\, g_A^2\, \langle\mathbf{GT}\rangle^2}, \tag{33}$$

where $g_A = 1.2723$ is the current experimental value [13] for the nucleon axial coupling constant, $\delta_R = 1.9\%$ is the outer radiative correction [14], t is the half-life of ^{3}H, and f_V and f_A are Fermi functions reported in Ref. [15] to have the values 2.8355×10^{-6} and 2.8505×10^{-6}, respectively. The experimental value used for K/G_V^2 is (6144.5 ± 1.9) s as obtained from Ref. [16], and that used for $(1 + \delta_R)\, t\, f_V$ is (1134.6 ± 3.1) s as reported in Ref. [15]. Finally, $\langle\mathbf{F}\rangle$ and

TABLE I. Contributions to the GT matrix element of tritium β decay corresponding to the Hamiltonian model N3LO/N2LO (AV18/UIX) and cutoffs $\Lambda = 500$ MeV and 600 MeV in the chiral potentials and weak axial current operators. The acronyms LO, N2LO, N3LO(OPE), N3LO(CT), N4LO(OPE), N4LO(MPE), and N4LO(3Ba) refer, respectively, to the axial operators given in Eqs. (12), (13), (14), (15), (16), (17), and (A11). In the N3LO(OPE) operator the LECs c_3 and c_4 have the values $c_3 = -3.20\,\mathrm{GeV}^{-1}$ and $c_4 = 5.40\,\mathrm{GeV}^{-1}$ from Refs. [18,19], while in the N3LO*(OPE) operator they are taken as $c_3 = -5.61\,\mathrm{GeV}^{-1}$ and $c_4 = 4.26\,\mathrm{GeV}^{-1}$ from Ref. [24]. The LEC z_0 in N3LO(CT) is taken to have the value $z_0 = 1$ in units of GeV^{-3}. The LECs (c_D,c_E) in the three-nucleon chiral potential have the values $(-1.847, -0.548)$ for $\Lambda = 500$ MeV and $(-2.030, -1.553)$ for $\Lambda = 600$ MeV. See text for further explanations.

Λ	500 MeV	600 MeV
LO	0.9363(0.9224)	0.9322 (0.9224)
N2LO	$-0.569(-0.844)\times10^{-2}$	$-0.457(-0.844)\times10^{-2}$
N3LO(OPE)	$0.825(1.304)\times10^{-2}$	$0.043(7.517)\times10^{-2}$
N3LO*(OPE)	$0.579(0.812)\times10^{-1}$	$0.652(1.413)\times10^{-1}$
N3LO(CT)	$-0.586(-0.721)\times10^{-3}$	$-0.717(-0.644)\times10^{-3}$
N4LO(OPE)	$-0.697(-0.964)\times10^{-2}$	$-0.867(-1.216)\times10^{-2}$
N4LO(MPE)	$-0.430(-0.565)\times10^{-1}$	$-0.532(-0.775)\times10^{-1}$
N4LO(3Ba)	$-0.143(-0.183)\times10^{-2}$	$-0.153(-0.205)\times10^{-2}$

$\langle\mathbf{GT}\rangle$ denote the reduced matrix element of the Fermi (F) and GT operators. The GT operator is the axial current constructed in Sec. III. The F operator is the vector charge and, while it too includes one- and two-body terms derived in Ref. [9], the latter vanish in the limit of vanishing external field momentum, and only the one-body term at LO contributes in this limit.

The F and GT matrix elements are calculated with ^{3}H and ^{3}He wave functions obtained with the hyperspherical-harmonics (HH) expansion method (see review [17]) from two- and three-nucleon potentials derived from either χEFT or the conventional approach. The combination of chiral potentials is denoted as N3LO/N2LO(500) [N3LO/N2LO(600)] corresponding to cutoff $\Lambda = 500$ MeV ($\Lambda = 600$ MeV), and consists of two-nucleon potentials at N3LO from Refs. [18,19] and three-nucleon potentials at N2LO from Refs. [20,21].[1] The combination of conventional potentials is denoted as AV18/UIX and consists of the Argonne v_{18} (AV18) two-nucleon potential [22] and Urbana-IX (UIX) three-nucleon potential [23]. In all cases we obtain $\langle\mathbf{F}\rangle = 0.9998$. From this value we extract via Eq. (33) the experimental GT matrix element as

$$\mathrm{GT}_{\mathrm{EXP}} = \langle\mathbf{GT}\rangle_{\mathrm{EXP}}/\sqrt{3} = 0.9511 \pm 0.0013. \qquad (34)$$

Contributions to the GT matrix element corresponding to the LO, N2LO, N3LO, N4LO, and N4LO(3Ba) axial operators are reported in Table I, where the LEC z_0 in the N3LO(CT) operator is taken as $z_0 = 1$ in units of GeV^{-3}. The LECs c_3 and c_4 in the N3LO(OPE) operators are constrained by fits to πN scattering data, and two different sets of values (listed in the table caption) have been used in the present study, one from Refs. [18,19] and the other from a recent analysis of these data based on Roy-Steiner equations [24], specifically the values corresponding to the column labeled N3LO in Table II of that work. The first set of c_3 and c_4 values (from Refs. [18,19]) enters the chiral two- and three-nucleon potentials, used here to generate the ^{3}H and ^{3}He wave functions. Clearly, use of the second set from Ref. [24] in the N3LO(OPE) axial current is not consistent with these potentials; results for the GT matrix element are provided in that case only to give an estimate of the their sensitivity to the c_3 and c_4 values. As per the additional LECs (c_D,c_E) in the three-nucleon potential, these have been obtained by the fitting procedure described below. In particular, we note that the LEC z_0 in the N3LO(CT) operator is related to c_D via Eq. (37).

TABLE II. Adimensional values of the LECs corresponding to the AV18/UIX Hamiltonian model and cutoffs $\Lambda = 500$ MeV and 600 MeV in the chiral axial current. The LEC $\hat{z}_0$ is determined by reproducing $\mathrm{GT}_{\mathrm{EXP}}$ in calculations including in this current corrections up to either N3LO or N4LO. The values for $\hat{z}_0$, $\hat{d}_R$, and c_D are obtained using the LECs $(c_3,c_4) = (-3.20,5.40)\ \mathrm{GeV}^{-1}$ from Refs. [18,19], those for $\hat{z}_0^\star$, $\hat{d}_R^\star$, and $c_D^\star$ using $(c_3,c_4) = (-5.61,4.26)\ \mathrm{GeV}^{-1}$ from Ref. [24], in both the N3LO and N4LO calculations.

	N3LO		N4LO	
Λ	500	600	500	600
$\hat{z}_0$	−0.421	0.742	−1.607	−1.048
$\hat{d}_R$	2.122	3.285	0.936	1.495
c_D	−0.571	1.007	−2.180	−1.421
$\hat{z}_0^\star$	0.769	2.038	−0.417	0.235
$\hat{d}_R^\star$	1.850	3.115	0.660	1.311
$c_D^\star$	1.043	2.764	−0.566	0.318

In the N4LO(3Ba) current we have only considered the term $\mathbf{j}_\pm^{\mathrm{N4LO}}(3\mathrm{B,a})$ of Eq. (A11) and neglected the term $\mathbf{j}_\pm^{\mathrm{N4LO}}(3\mathrm{B,b})$ of Eq. (A17) for reasons explained in Appendix. The GT (and F) matrix elements are computed exactly, without approximation, with quantum Monte Carlo methods. The spin-isospin algebra is carried out with techniques similar to those developed in Ref. [25] for the electromagnetic current operator. The results reported in the tables below are based on random walks consisting of 10^6 configurations. Statistical errors are not listed, but are typically at the few parts in 10^3, except in the special case of the N3LO(OPE) results, for which they are at the few % level (see below).

In Table I we report the results for the N3LO/N2LO(500) and N3LO/N2LO(600) models, and in parentheses those for the AV18/UIX model. The LO and N2LO axial operators do not need to be regularized, and hence the corresponding contributions for the AV18/UIX are the same for $\Lambda = 500$ MeV and 600 MeV. However, the N3LO/N2LO contributions change (rather significantly at N2LO) as Λ varies in this range due to the intrinsic cutoff dependence of the potentials. In the N3LO axial current of Eq. (14) the

[1]Note that for consistency with the convention adopted in Fig. 1, it would be more appropriate to label these two- and three-nucleon potentials, respectively, as N4LO and N3LO. However, this is not the standard notation used in the literature.

terms proportional to c_3 and c_4 have opposite signs and tend to cancel each other. This cancellation depends crucially on the values of the LECs and Hamiltonian model. In particular, when c_3 and c_4 are taken from Refs. [18,19], the sum of their contributions for the N3LO/N2LO model is (in magnitude) comparable to the contribution from the nonlocal terms proportional to $\mathbf{K}_i$ in Eq. (14).

The contributions from loop corrections, row labeled N4LO(MPE), are relatively large and comparable to those at N3LO(OPE). As a matter of fact, when the values for the c_3 and c_4 LECs are from Refs. [18,19], the N3LO(OPE) contributions are an order of magnitude smaller than the N4LO(MPE) in the case of the chiral potentials. The origin of this large contribution can be traced back to the term proportional to the loop function $W_1(k)$ in Eq. (17), specifically to the term with the factor $(1-5\,g_A^2)$ in Eq. (18). It originates from box diagrams, panel (m) of Fig. 1 (see Ref. [1]). All the N4LO corrections have opposite signs relative to the LO and N3LO(OPE).

Next, we discuss the determination of the value for the LEC z_0 required to reproduce $\mathrm{GT_{EXP}}$ for the various Hamiltonian models we consider, by retaining corrections in the axial current up to either N3LO or N4LO. In order to compare with previous determinations of this LEC [4–6], we define an adimensional $\hat{z}_0$ by rescaling z_0 as

$$\hat{z}_0 = \frac{2\,m\,f_\pi^2}{g_A}\,z_0. \tag{35}$$

This $\hat{z}_0$ is simply given by $\hat{z}_0 = \hat{d}_1 + 2\,\hat{d}_2$ in terms of the LECs $\hat{d}_1$ and $\hat{d}_2$ introduced in Ref. [4] (in [4] these LECs multiply contact axial currents related to each other by a Fierz rearrangement, and are not therefore independent). We also note the relation

$$\hat{d}_R = \hat{z}_0 + \frac{\hat{c}_3}{3} + \frac{2\,\hat{c}_4}{3} + \frac{1}{6}, \tag{36}$$

where $\hat{c}_i = m\,c_i$ are adimensional, and $\hat{d}_R$ was fixed in Ref. [4] by fitting $\mathrm{GT_{EXP}}$ in a hybrid calculation based on the AV18/UIX model and including N3LO corrections in the axial current.

Lastly, the LEC c_D in the three-nucleon potential at N2LO is related to $\hat{z}_0$ via [4–6]

$$c_D = \frac{g_A\,\Lambda_\chi}{m}\hat{z}_0, \tag{37}$$

where Λ_χ is taken as 1 GeV here, while in Refs. [5,6] $\Lambda_\chi = 0.7$ GeV was adopted (Λ_χ is not to be confused with the cutoff Λ which regularizes the configuration-space expressions of the axial operators).

Values for the LECs are reported in Table II for the hybrid calculation based on the AV18/UIX Hamiltonian model, and in Table III for the chiral Hamiltonian model. In Table II the values for the various combinations considered above are listed, so that they can be compared with previous determinations [4,6,26]: they follow simply from reproducing the central value of $\mathrm{GT_{EXP}}$ in Eq. (34). In order to determine the values corresponding to the chiral potentials, we proceed as in Ref. [6]. The ^{3}H and ^{3}He ground state wave functions are calculated using these potentials for $\Lambda = 500$ MeV and 600 MeV. We span the range $c_D \in [-4,3]$, and, in correspondence to each c_D in this range, determine c_E so as to reproduce the binding energies of either ^{3}H or ^{3}He. The resulting trajectories are essentially indistinguishable, as shown in Fig. 4 for $\Lambda = 500$ MeV and in Fig. 5 for $\Lambda = 600$ MeV, and as already obtained in Ref. [6]. Then, for each set of (c_D,c_E), the triton and ^{3}He wave functions are calculated and the Gamow-Teller matrix element, denoted as $\mathrm{GT_{TH}}$, is determined, by including in the axial current corrections up to N3LO or N4LO. The ratio $\mathrm{GT_{TH}/GT_{EXP}}$ for both values of the cutoff Λ is shown in Fig. 6 for the N3LO case and Fig. 7 for the N4LO one. The LECs (c_D,c_E) that reproduce $\mathrm{GT_{EXP}}$ (its central value) and the trinucleon binding energies are given in Table III. The values for c_D at N3LO are found to be consistent with those listed in [6], after allowance is made for the different Λ_χ (0.7 GeV in that work versus 1

TABLE III. Values for the (c_D,c_E) LECs as obtained by fitting the $A = 3$ binding energy and $\mathrm{GT_{EXP}}$ (its central value), using the N3LO/N2LO potential models with cutoffs $\Lambda = 500$ MeV and 600 MeV. The results labeled N3LO and N4LO are obtained retaining in the nuclear axial current up to N3LO and N4LO contributions, respectively.

	N3LO		N4LO	
Λ	500	600	500	600
c_D	−0.353	−0.443	−1.847	−2.030
c_E	−0.305	−1.224	−0.548	−1.553

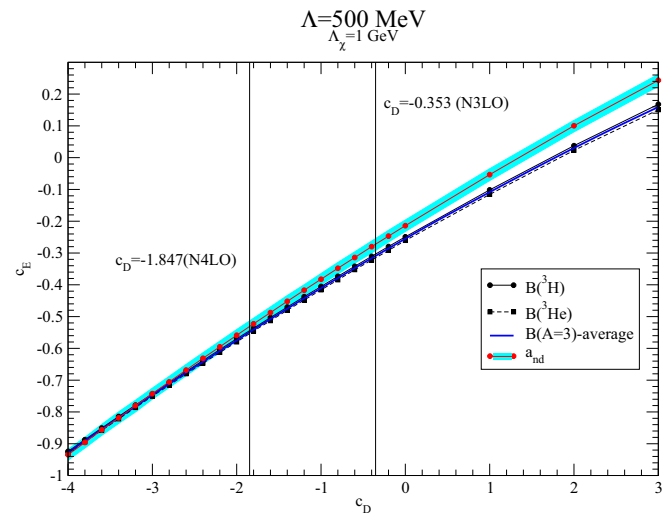

FIG. 4. The c_D–c_E trajectories fitted to reproduce the experimental $A = 3$ binding energies and the doublet nd scattering length using the N3LO/N2LO potential with $\Lambda = 500$ MeV. The values of 8.475 MeV, 7.725 MeV, and 0.645 ± 0.010 fm [27] are used for the ^{3}H, ^{3}He, and nd scattering length, respectively. Note that the $A = 3$ binding energies have been corrected for the small contributions (+7 keV in ^{3}H and −7 keV in ^{3}He) due to the $n-p$ mass difference [28]. The (cyan) band is due to the experimental uncertainty on the nd scattering length. The vertical lines indicate the c_D values obtained by fitting $\mathrm{GT_{EXP}}$ and retaining N4LO or only N3LO contributions in the axial current are also displayed.

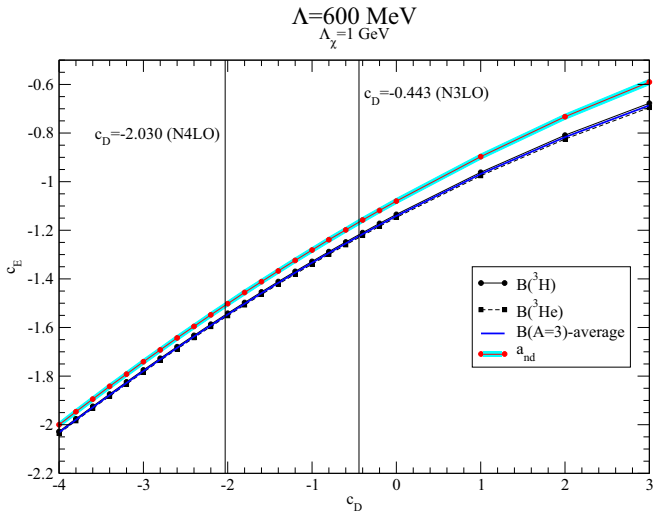

FIG. 5. Same as Fig. 4 but for $\Lambda = 600$ MeV.

GeV above) and for the fact that GT_{EXP} as determined here is slightly smaller than adopted in [6].

Alternatively, we could choose a different set of three-nucleon observables to fit these LECs. We consider here, together with the $A = 3$ binding energy, the nd doublet scattering length a_{nd}, for which we take the experimental value 0.645 ± 0.010 fm, obtained in Ref. [27]. In the range $c_D \in [-4,3]$ the resulting trajectories are displayed in Figs. 4 and 5 for $\Lambda = 500$ MeV and 600 MeV, respectively. The experimental uncertainty in a_{nd} has been taken into account, and therefore the results of Figs. 4 and 5 are presented as a band. The trajectories originating from the $A = 3$ binding energies and nd scattering length are quite close to each other, but do not overlap. In the $\Lambda = 500$ MeV case, there is a crossing point at $(c_D, c_E) = (-2.340, -0.567)$, while for $\Lambda = 600$ MeV there is no crossing. In particular, using the (c_D, c_E) in Table III, we obtain $a_{nd} = 0.654(0.665)$ fm for $\Lambda = 500$ MeV and $a_{nd} = 0.687(0.699)$ fm for $\Lambda = 600$ MeV, when the N4LO (N3LO) contributions in the axial current

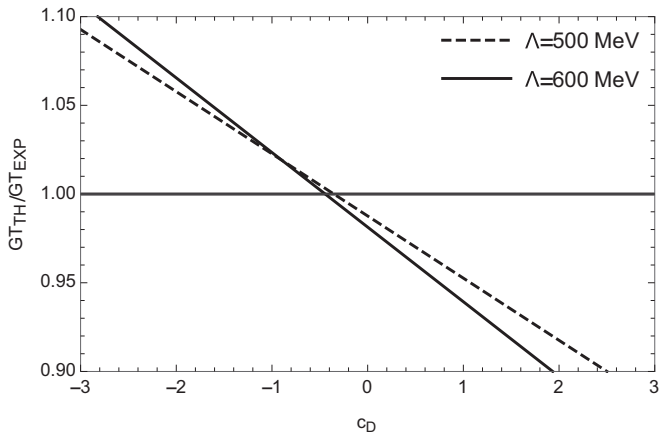

FIG. 6. The ratio GT_{TH}/GT_{EXP} as function of the LEC c_D obtained retaining corrections up to N3LO in the nuclear axial current. The results for both values of the cutoff Λ are shown.

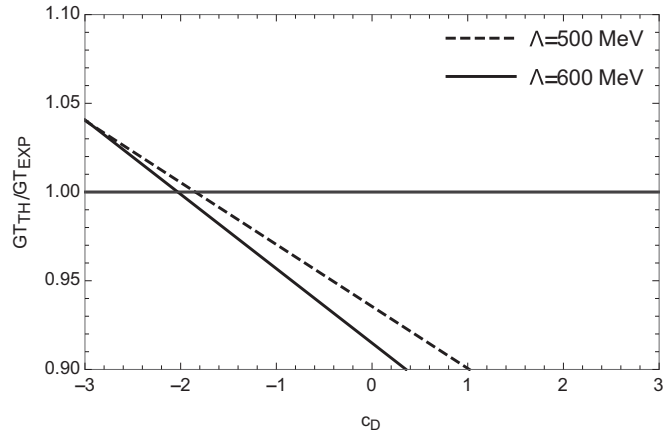

FIG. 7. Same as Fig. 6 but with the corrections in the axial current up to N4LO.

are retained. The present calculations of the nd scattering wave functions ignore higher order electromagnetic interaction terms, such as those associated with the nucleons' magnetic moments. These terms are known to reduce the a_{nd} value of about 3% [17], when the AV18/UIX Hamiltonian model is used. Thus, the present analysis seems to indicate that the three $A = 3$ observables ($A = 3$ binding energies, GT_{EXP}, and a_{nd}) are simultaneously reproduced, at least for $\Lambda = 500$ MeV, when the nuclear axial current retains corrections up to N4LO.

V. CONCLUSIONS

To summarize, in the present work we have carried out a calculation of the F and GT matrix elements in ^{3}H β decay with the charge-changing weak current recently derived in χEFT up to N4LO (one loop). The trinucleon wave functions have been obtained from accurate hyperspherical harmonics solutions of the Schrödinger equation corresponding to either chiral (N3LO/N2LO) or conventional (AV18/UIX) nuclear potentials, and the relevant matrix elements have been computed by Monte Carlo integration methods without any approximations (statistical errors are typically at the level of a few parts in 10^3).

We find that the OPE contributions at N3LO proportional to c_3 and c_4 interfere destructively and therefore depend strongly on the values of these LECs. As a consequence, the N4LO contributions turn out to be comparable (in magnitude) to the N3LO ones, even though nominally they are suppressed by a factor of Q/Λ_χ relative to N3LO. This leads to a strong variation of the LEC z_0 as determined respectively at N3LO or at N4LO. It is possible that the convergence of the chiral series is not satisfactory for this observable and that the effective theory should be enlarged to include explicit Δ's. An additional caveat is that, strictly speaking, the N4LO axial current calculations reported here should have involved the three-nucleon interaction at N3LO, whereas only the N2LO component has been considered in this work. Furthermore, the definition of the current operator is closely related to the prescription adopted for defining the nuclear potential off the energy-shell [1]. Whether different prescriptions lead to the same convergence pattern is a question that would require further investigation.

Finally, the LEC multiplying the contact axial current is related to the LEC c_D in the three-nucleon potential. This c_D and the other LEC c_E which fully characterize this (contact) potential have been constrained by a simultaneous fit to the empirical values of the three-nucleon binding energies and GT matrix element. When the fit is carried out in a calculation including the axial current at N4LO, the resulting c_D and c_E also lead to a doublet nd scattering length in reasonable agreement with the experimental value for $\Lambda = 500$ MeV.

ACKNOWLEDGMENTS

An email exchange with B. Kubis in reference to the c_i LECs is gratefully acknowledged. This research is supported by the U.S. Department of Energy, Office of Nuclear Physics, under Contract No. DE-AC05-06OR23177 (A.B. and R.S.). A.B. was supported by a Jefferson Science Associates Theory Fellowship.

APPENDIX: CONFIGURATION-SPACE EXPRESSIONS

The Fourier transforms of two-body operators are easily reduced to one-dimensional integrals [or two-dimensional ones in the case of the N4LO(MPE) operator], which are then evaluated by Gaussian quadrature formulas. For example, the N3LO(OPE) current is given by

$$\mathbf{j}_{\pm}^{\rm N3LO}({\rm OPE}) = \mathbf{j}_{\pm}^{\rm N3LO}(c_3) + \mathbf{j}_{\pm}^{\rm N3LO}(c_4) + \mathbf{j}_{\pm}^{\rm N3LO}({\rm nl}), \tag{A1}$$

where

$$\mathbf{j}_{\pm}^{\rm N3LO}(c_3) = -\tau_{2,\pm}\left[\frac{F_1(z;c_3)}{z}\,\boldsymbol{\sigma}_2 + F_2(z;c_3)\,\hat{\mathbf{z}}\,(\boldsymbol{\sigma}_2\cdot\hat{\mathbf{z}})\right] + (1 \rightleftharpoons 2), \tag{A2}$$

$$\mathbf{j}_{\pm}^{\rm N3LO}(c_4) = -(\boldsymbol{\tau}_1\times\boldsymbol{\tau}_2)_{\pm}\,\boldsymbol{\sigma}_1\times\left[\frac{F_1(z;c_4)}{z}\,\boldsymbol{\sigma}_2 + F_2(z;c_4)\,\hat{\mathbf{z}}\,(\boldsymbol{\sigma}_2\cdot\hat{\mathbf{z}})\right] + (1 \rightleftharpoons 2), \tag{A3}$$

$$\mathbf{j}_{\pm}^{\rm N3LO}({\rm nl}) = -(\boldsymbol{\tau}_1\times\boldsymbol{\tau}_2)_{\pm}\left\{-i\,\boldsymbol{\nabla}_1^z,\, F_1(z;{\rm nl})\,\boldsymbol{\sigma}_2\cdot\hat{\mathbf{z}}\right\} + (1 \rightleftharpoons 2). \tag{A4}$$

Here we have defined $\mathbf{r} = \mathbf{r}_1 - \mathbf{r}_2$, the adimensional variable $\mathbf{z} = \Lambda\,\mathbf{r}$, $-i\,\boldsymbol{\nabla}_i^z$ as the adimensional momentum operator, and the radial functions

$$F_1(z;c_3) = -\frac{1}{\pi^2}\,\frac{g_A\,\overline{c}_3}{\overline{f}_\pi^2}\int_0^\infty dx\,\frac{x^3}{x^2+\overline{m}_\pi^2}\,{\rm e}^{-x^4}\,j_1(xz), \tag{A5}$$

$$F_2(z;c_3) = \frac{1}{\pi^2}\,\frac{g_A\,\overline{c}_3}{\overline{f}_\pi^2}\int_0^\infty dx\,\frac{x^4}{x^2+\overline{m}_\pi^2}\,{\rm e}^{-x^4}\,j_2(xz), \tag{A6}$$

where $j_n(xz)$ are spherical Bessel functions. We have also introduced adimensional constants (denoted with the overline) expressing them units of the cutoff Λ. They are given by

$$\overline{m}_\pi = m_\pi/\Lambda, \quad \overline{m} = m/\Lambda, \quad \overline{f}_\pi = f_\pi/\Lambda, \quad \overline{c}_3 = c_3\,\Lambda, \quad \overline{c}_4 = c_4\,\Lambda. \tag{A7}$$

The functions $F_1(z;c_4)$ and $F_2(z;c_4)$, and $F_1(z;{\rm nl})$ follow from those above by the replacement of the prefactor as

$$\frac{1}{\pi^2}\,\frac{g_A\,\overline{c}_3}{\overline{f}_\pi^2} \longrightarrow \frac{1}{4\,\pi^2}\,\frac{g_A}{\overline{f}_\pi^2}\left(\overline{c}_4 + \frac{1}{4\,\overline{m}}\right) \quad \text{for} \quad F_1(z;c_4) \quad \text{and} \quad F_2(z;c_4), \tag{A8}$$

$$\frac{1}{\pi^2}\,\frac{g_A\,\overline{c}_3}{\overline{f}_\pi^2} \longrightarrow \frac{1}{16\,\pi^2}\,\frac{g_A}{\overline{m}\,\overline{f}_\pi^2} \quad \text{for} \quad F_1(z;{\rm nl}). \tag{A9}$$

The Fourier transform of the three-body operator is more involved. We express it as

$$\mathbf{j}_{\pm}^{\rm N4LO}({\rm 3B}) = \mathbf{j}_{\pm}^{\rm N4LO}({\rm 3B,a}) + \mathbf{j}_{\pm}^{\rm N4LO}({\rm 3B,b}), \tag{A10}$$

where

$$\mathbf{j}_{\pm}^{\rm N4LO}({\rm 3B,a}) = \sum_{\rm cyc}(2\,\tau_{1,\pm}\,\boldsymbol{\tau}_2\cdot\boldsymbol{\tau}_3 - \tau_{2,\pm}\,\boldsymbol{\tau}_3\cdot\boldsymbol{\tau}_1 - \tau_{3,\pm}\,\boldsymbol{\tau}_1\cdot\boldsymbol{\tau}_2) \times\boldsymbol{\sigma}_1(\boldsymbol{\sigma}_2\cdot\hat{\mathbf{z}}_{12})(\boldsymbol{\sigma}_3\cdot\hat{\mathbf{z}}_{13})F_1(z_{12};{\rm 3B})\,F_1(z_{13};{\rm 3B}), \tag{A11}$$

and the function $F_1(z;\mathrm{3B})$ is obtained from $F_1(z;c_3)$ by replacing

$$\frac{1}{\pi^2}\,\frac{g_A\,\overline{c}_3}{\overline{f}_\pi^{\,2}} \longrightarrow \frac{1}{4\sqrt{2}\,\pi^2}\,\frac{g_A^{3/2}}{\overline{f}_\pi^{\,2}}. \tag{A12}$$

In order to reduce the Fourier transform of the b term in the N4LO(3B) current to a two-dimensional parametric integral, we first regularize it as

$$\mathbf{j}_\pm^{\mathrm{N4LO}}(\mathbf{k}_2,\mathbf{k}_3;\mathrm{3B,b}) = \sum_{\mathrm{cyc}} \frac{g_A^3}{6\,f_\pi^4}(\mathrm{isospin})\;\boldsymbol{\sigma}_3\cdot\boldsymbol{\nabla}_3\;\boldsymbol{\sigma}_2\cdot\boldsymbol{\nabla}_2\;\boldsymbol{\sigma}_1\cdot\boldsymbol{\nabla}_1\;\boldsymbol{\nabla}_1\;I, \tag{A13}$$

$$I = \int \frac{d\mathbf{k}_2}{(2\pi)^3}\,\frac{d\mathbf{k}_3}{(2\pi)^3}\,C_\Lambda(|\,\mathbf{k}_2+\mathbf{k}_3\,|)\,\mathrm{e}^{-i(\mathbf{k}_2\cdot\mathbf{r}_{12}+\mathbf{k}_3\cdot\mathbf{r}_{13})}\,\frac{1}{\omega^2_{\mathbf{k}_2+\mathbf{k}_3}\,\omega^2_{\mathbf{k}_2}\,\omega^2_{\mathbf{k}_3}}, \tag{A14}$$

where (isospin) stands for the isospin factor in parentheses of Eq. (A11). After changing variables to $\mathbf{k}_2=\mathbf{P}/2+\mathbf{p}$ and $\mathbf{k}_3=\mathbf{P}/2-\mathbf{p}$, making use of Feynman's parametrization for the denominator $1/(\omega_{\mathbf{P}/2+\mathbf{k}}\,\omega_{\mathbf{P}/2-\mathbf{k}})$, and carrying out the angular integration over the $\mathbf{P}$ directions, we find

$$I = \frac{1}{16\pi^3}\int_{-1/2}^{1/2} dy \int_0^\infty d\,P\;P^2\,\frac{\mathrm{e}^{-(P/\Lambda)^4}}{P^2+m_\pi^2}\,j_0(P\,|\,\mathbf{r}_1-\mathbf{R}_{23}+y\,\mathbf{r}_{23}\,|)\mathrm{e}^{-L(P,y)\,r_{23}}\,\frac{1}{L(P,y)}, \tag{A15}$$

where

$$L(P,y) = \sqrt{m_\pi^2+P^2(1/4-y^2)}. \tag{A16}$$

In terms of adimensional variables, the current now reads

$$\begin{aligned}\mathbf{j}_\pm^{\mathrm{N4LO}}(\mathrm{3B,b}) = \sum_{\mathrm{cyc}} \frac{g_A^3}{96\,\pi^3\,\overline{f}_\pi^4}(\mathrm{isospin})\;\boldsymbol{\sigma}_3\cdot\boldsymbol{\nabla}_3^z\;\boldsymbol{\sigma}_2\cdot\boldsymbol{\nabla}_2^z\;\boldsymbol{\sigma}_1\cdot\boldsymbol{\nabla}_1^z\;\boldsymbol{\nabla}_1^z\int_{-1/2}^{1/2}dy\int_0^\infty dx\,x^2\,\frac{\mathrm{e}^{-x^4}}{x^2+\overline{m}_\pi^2}\\ \times\frac{\mathrm{e}^{-\overline{L}(x,y)\,z}}{\overline{L}(x,y)}\;j_0(x\,|\,\mathbf{Z}+y\,\mathbf{z}\,|),\end{aligned} \tag{A17}$$

where the gradients are relative to $\mathbf{z}_i=\Lambda\,\mathbf{r}_i$, and we have defined $\mathbf{Z}=\Lambda(\mathbf{r}_1-\mathbf{R}_{23})$ and $\mathbf{z}=\Lambda\,\mathbf{r}_{23}$, and

$$\overline{L}(x,y) = \sqrt{\overline{m}_\pi^2+x^2(1/4-y^2)}. \tag{A18}$$

In order to evaluate the gradients, we introduce the Jacobi variables,

$$\boldsymbol{\nabla}_1^z=\boldsymbol{\nabla}^Z,\quad \boldsymbol{\nabla}_2^z=-\frac{1}{2}\boldsymbol{\nabla}^Z+\boldsymbol{\nabla}^z,\qquad \boldsymbol{\nabla}_3^z=-\frac{1}{2}\boldsymbol{\nabla}^Z-\boldsymbol{\nabla}^z, \tag{A19}$$

where the gradients $\boldsymbol{\nabla}^Z$ and $\boldsymbol{\nabla}^z$ are now relative to $\mathbf{Z}$ and $\mathbf{z}$, respectively. We obtain

$$\begin{aligned}&\sigma_{3,\delta}\,\sigma_{2,\gamma}\,\sigma_{1,\beta}\left(\frac{1}{4}\nabla_\delta^Z\nabla_\gamma^Z-\nabla_\delta^z\nabla_\gamma^z-\frac{1}{2}\nabla_\delta^Z\nabla_\gamma^z+\frac{1}{2}\nabla_\delta^z\nabla_\gamma^Z\right)\left[\mathrm{e}^{-\overline{L}z}\;\nabla_\beta^Z\nabla_\alpha^Z\;j_0(x\,|\,\mathbf{Z}+y\,\mathbf{z}\,|)\right]\\ &=x^2\,\mathrm{e}^{-\overline{L}z}\,\sigma_{3,\delta}\,\sigma_{2,\gamma}\,\sigma_{1,\beta}\left\{x^2\left(\frac{1}{4}-y^2\right)\nabla_\delta^t\nabla_\gamma^t\nabla_\beta^t\nabla_\alpha^t-x\,\overline{L}\left(\frac{1}{2}-y\right)\hat{z}_\delta\nabla_\gamma^t\nabla_\beta^t\nabla_\alpha^t\right.\\ &\left.+x\,\overline{L}\left(\frac{1}{2}+y\right)\hat{z}_\gamma\nabla_\delta^t\nabla_\beta^t\nabla_\alpha^t-\left[\overline{L}^2\left(1+\frac{1}{\overline{L}z}\right)\hat{z}_\delta\,\hat{z}_\gamma-\frac{\overline{L}}{z}\delta_{\gamma\delta}\right]\nabla_\beta^t\nabla_\alpha^t\right\}j_0(t),\end{aligned} \tag{A20}$$

where we have defined $\mathbf{t}=x\,\mathbf{Z}+x\,y\,\mathbf{z}$ and the corresponding gradient $\boldsymbol{\nabla}^t$. By making use of the identities

$$\nabla_\beta^t\nabla_\alpha^t\,j_0(t) = \delta_{\alpha\beta}\left(\frac{1}{t}\frac{d}{dt}\right)j_0(t)+t_\alpha\,t_\beta\left(\frac{1}{t}\frac{d}{dt}\right)^2 j_0(t), \tag{A21}$$

$$\nabla_\gamma^t\nabla_\beta^t\nabla_\alpha^t\,j_0(t) = \left(\delta_{\alpha\beta}\,t_\gamma+\delta_{\alpha\gamma}\,t_\beta+\delta_{\beta\gamma}\,t_\alpha\right)\left(\frac{1}{t}\frac{d}{dt}\right)^2 j_0(t)+t_\alpha\,t_\beta\,t_\gamma\left(\frac{1}{t}\frac{d}{dt}\right)^3 j_0(t), \tag{A22}$$

$$\begin{aligned}\nabla_\delta^t\nabla_\gamma^t\nabla_\beta^t\nabla_\alpha^t\,j_0(t) &= \left(\delta_{\alpha\beta}\,\delta_{\gamma\delta}+\delta_{\alpha\gamma}\,\delta_{\beta\delta}+\delta_{\beta\gamma}\,\delta_{\alpha\delta}\right)\left(\frac{1}{t}\frac{d}{dt}\right)^2 j_0(t)+\left(\delta_{\alpha\beta}\,t_\gamma\,t_\delta+\delta_{\alpha\gamma}\,t_\beta\,t_\delta\right.\\ &\left.+\delta_{\beta\gamma}\,t_\alpha\,t_\delta+\delta_{\alpha\delta}\,t_\beta\,t_\gamma+\delta_{\beta\delta}\,t_\alpha\,t_\gamma+\delta_{\gamma\delta}\,t_\alpha\,t_\beta\right)\left(\frac{1}{t}\frac{d}{dt}\right)^3 j_0(t)+t_\alpha\,t_\beta\,t_\gamma\,t_\delta\left(\frac{1}{t}\frac{d}{dt}\right)^4 j_0(t),\end{aligned} \tag{A23}$$

and

$$\left(\frac{1}{t}\frac{d}{dt}\right)^m j_0(t) = (-)^m \frac{1}{t^m}\, j_m(t), \tag{A24}$$

the current in Eq. (A17) is reduced to a sum of terms depending on parametric integrals in x and y. While the matrix element of $\mathbf{j}^{\mathrm{N4LO}}(3\mathrm{B},\mathrm{b})$ could in principle be evaluated, the computational effort required to do so in the present Monte Carlo calculations is, however, too large (and unjustified in view of its expected contribution, see Table I). For this reason it has been neglected in the present study.

[1] A. Baroni, L. Girlanda, S. Pastore, R. Schiavilla, and M. Viviani, Phys. Rev. C **93**, 015501 (2016); **93**, 049902(E) (2016).
[2] N. Fettes, U.-G. Meissner, M. Mojzis, and S. Steininger, Ann. Phys. (NY) **283**, 273 (2000).
[3] T.-S. Park, D.-P. Min, and M. Rho, Phys. Rep. **233**, 341 (1993).
[4] T.-S. Park, L. E. Marcucci, R. Schiavilla, M. Viviani, A. Kievsky, S. Rosati, K. Kubodera, D.-P. Min, and M. Rho, Phys. Rev. C **67**, 055206 (2003).
[5] D. Gazit, S. Quaglioni, and P. Navratil, Phys. Rev. Lett. **103**, 102502 (2009).
[6] L. E. Marcucci, A. Kievsky, S. Rosati, R. Schiavilla, and M. Viviani, Phys. Rev. Lett. **108**, 052502 (2012).
[7] L. E. Marcucci, R. Schiavilla, and M. Viviani, Phys. Rev. Lett. **110**, 192503 (2013).
[8] P. Klos, J. Menendez, D. Gazit, and A. Schwenk, Phys. Rev. D **88**, 083516 (2013).
[9] S. Pastore, L. Girlanda, R. Schiavilla, and M. Viviani, Phys. Rev. C **84**, 024001 (2011).
[10] J. L. Friar, Ann. Phys. (NY) **104**, 380 (1977).
[11] M. Piarulli, L. Girlanda, L. E. Marcucci, S. Pastore, R. Schiavilla, and M. Viviani, Phys. Rev. C **87**, 014006 (2013).
[12] R. Schiavilla, V. G. J. Stoks, W. Glöckle, H. Kamada, A. Nogga, J. Carlson, R. Machleidt, V. R. Pandharipande, R. B. Wiringa, A. Kievsky, S. Rosati, and M. Viviani, Phys. Rev. C **58**, 1263 (1998).
[13] K. A. Olive *et al.* (Particle Data Group), Chin. Phys. C **38**, 090001 (2014).
[14] S. Raman, C. A. Houser, T. A. Walkiewicz, and I. S. Towner, At. Data Nucl. Data Tables **21**, 567 (1978).
[15] J. J. Simpson, Phys. Rev. C **35**, 752 (1987).
[16] J. C. Hardy and I. S. Towner, Phys. Rev. C **91**, 025501 (2015).
[17] A. Kievsky, S. Rosati, M. Viviani, L. E. Marcucci, and L. Girlanda, J. Phys. G: Nucl. Part. Phys. **35**, 063101 (2008).
[18] D. R. Entem and R. Machleidt, Phys. Rev. C **68**, 041001(R) (2003).
[19] R. Machleidt and D. R. Entem, Phys. Rep. **503**, 1 (2011).
[20] E. Epelbaum, A. Nogga, W. Glöckle, H. Kamada, Ulf-G. Meißner, and H. Witala, Phys. Rev. C **66**, 064001 (2002).
[21] P. Navrátil, Few-Body Syst. **41**, 117 (2007).
[22] R. B. Wiringa, V. G. J. Stoks, and R. Schiavilla, Phys. Rev. C **51**, 38 (1995).
[23] B. S. Pudliner, V. R. Pandharipande, J. Carlson, and R. B. Wiringa, Phys. Rev. Lett. **74**, 4396 (1995).
[24] M. Hoferichter, J. Ruiz de Elvira, B. Kubis, and Ulf-G. Meissner, Phys. Rev. Lett. **115**, 192301 (2015).
[25] R. Schiavilla, V. R. Pandharipande, and D. O. Riska, Phys. Rev. C **40**, 2294 (1989).
[26] L. E. Marcucci, M. Piarulli, M. Viviani, L. Girlanda, A. Kievsky, S. Rosati, and R. Schiavilla, Phys. Rev. C **83**, 014002 (2011).
[27] K. Schoen, D. L. Jacobson, M. Arif, P. R. Huffman, T. C. Black, W. M. Snow, S. K. Lamoreaux, H. Kaiser, and S. A. Werner, Phys. Rev. C **67**, 044005 (2003).
[28] A. Nogga, A. Kievsky, H. Kamada, W. Glöckle, L. E. Marcucci, S. Rosati, and M. Viviani, Phys. Rev. C **67**, 034004 (2003).